催化学报
2012 Chinese Journal of Catalysis Vol. 33 No. 10

Article ID: 0253-9837(2012)10-1672-09 **DOI**: 10.1016/S1872-2067(11)60446-4 **Article:** 1672–1680

LED Irradiation of a Photocatalyst for Benzene, Toluene, Ethyl Benzene, and Xylene Decomposition

JO Wan-Kuen*, KANG Hyun-Jung

Department of Environmental Engineering, Kyungpook National University, Daegu 702−701, Korea

Abstract: Studies on the use of gas phase applications of light emitting diodes (LEDs) in photocatalysis are scarce although their photocatalytic decomposition kinetics of environmental pollutants are likely different from those in aqueous solutions. The present study evaluated the use of chips of visible light LEDs to irradiate nitrogen doped titania (N-TiO_2) prepared by hydrolysis to decompose gaseous benzene, toluene, ethyl benzene, *m*-xylene, *p*-xylene, and *o*-xylene. Photocatalysts calcined at different temperatures were characterized by various analytical instruments. The degradation efficiency of benzene was close to zero for all conditions. For the other compounds, a conventional 8 W daylight lamp/N-TiO_2 unit gave a higher photocatalytic degradation efficiency as compared with that of visible-LED/N-TiO_2 units. However, the ratios of degradation efficiency to electric power consumption were higher for the photocatalytic units that used two types of visible-LED lamps (blue and white LEDs). The highest degradation efficiency was observed with the use of a calcination temperature of 350 °C. The average degradation efficiencies for toluene, ethyl benzene, *m*-xylene, *p*-xylene, and *o*-xylene were 35%, 68%, 94%, and 93%, respectively. The use of blue- and white-LEDs, high light intensity, and low initial concentrations gave high photocatalytic activities for the photocatalytic units using visible-LEDs. The morphological and optical properties of the photocatalysts were correlated to explain the dependence of photocatalytic activity on calcination temperature. The results suggest that visible-LEDs are energy efficient light source for photocatalytic gas phase applications, but the activity depends on the operational conditions.

Key words: light emitting diode; energy efficiency; gas phase degradation; photocatalyst characterization; calcination temperature

CLC number: O643 **Document code:** A

Received 22 July 2012. Accepted 20 August 2012.

**Corresponding author. Tel: +82-53-9506584; Fax: +82-53-9506579; E-mail: wkjo@knu.ac.kr*

This work was supported by the National Research Foundation of Korea (NRF) grant funded by the Korea government (MEST) (2011-0027916).

English edition available online at Elsevier ScienceDirect (http://www.sciencedirect.com/science/journal/18722067).

Heterogeneous photocatalysis is a promising technique for environmental pollutant purification by the oxidation of a variety of water and air pollutants with high efficiency. The process involves reactions with superoxide ions (O_2^-) and hydroxyl radicals (OH·) formed by photocatalytic processes when light is irradiated on the photocatalysts [1,2]. Titania (TiO_2) is the most used semiconductor photocatalyst because of its low cost, easy availability, and chemical stability [3,4]. However, this photocatalyst only exhibits reasonable activity under UV light (λ < 380 nm) whose energy exceeds the band gap energy of 3.2 eV. This limits its practical application [3]. Therefore, several methods of modifying TiO_2 have been used to increase visible light absorption efficiency and photocatalytic activity [2,5−7]. Techniques that have been tried include transition metal impregnation, dye sensitizing, and doping [8]. TiO_2 doped with nitrogen is one of the most promising photocatalysts that exhibit photosensitization in visible light [9,10]. With the N-impregnated method, N atoms are embedded into different sites of the TiO_2. These interstitial N atoms are likely charged and because of this they have visible light response [11]. Several studies have found that N-impregnated TiO_2 (N-TiO_2) exhibited high photocatalytic activity for environmental pollutants under visible light irradiation [5,12,13]. These studies utilized conventional lamps, such as the fluorescent daylight lamp and mercury-xenon lamp, as the visible light source.

Light emitting diodes (LEDs) have many merits over typical light sources and have been suggested as photocatalytic light sources. LEDs convert electric energy more efficiently into light because they have higher quantum yields, which are close to unity. They have long lifetimes, with a typical lifetime of 25000 to 100000 h [14]. In addition, LEDs provide a tunable and almost monochromatic light. These LED characteristics have led to the application of LEDs as alternative light sources to conventional lamps in photocatalytic processes for hydrogen generation [15,16] and environmental remediation [5,17−20]. A few studies have reported that UV-LED irradiated TiO_2 powder can remove liquid phase *o*-cresol [17] and 4-chlorophenol [18], and gas phase formaldehyde at a very high concentration (5%) [19]. Matsumoto et al. [5] and Liu et al. [20] have

investigated the feasibility of using visible-LED instead of UV-LED with doped titania to remove methyl orange in aqueous solution. However, unlike the aqueous phase applications, gas phase applications of visible-LEDs in photocatalytic studies are scarce in the literature, although the photocatalytic kinetics are likely to be different in the two phases. This study investigated the use of chips of visible-LED to irradiated nitrogen-doped titania (N-TiO_2) prepared by hydrolysis to decompose gas phase benzene, toluene, ethyl benzene, and xylene.

1 Experimental

1.1 Photocatalyst preparation

N-TiO_2 powder was prepared using a hydrolysis method [21]. Urea was utilized as a nitrogen source for N impregnation. The commercial TiO_2 powder (Degussa P25, 8 g) was transferred into 20 ml of an organic nitrogen solution. After stirring at room temperature for 1 h, this was stored in the dark for 24 h. Then, the mixture was dried under reduced pressure. The dried powder was calcined at 350, 450, 550, and 650 °C for 1 h to obtain a yellow N-doped TiO_2 powder. The calcined N-doped TiO_2 powder was washed with dilute sulfuric acid and pure water. Finally, the powder was dried under vacuum. The N-TiO_2 powder was characterized by a X-ray diffraction (XRD, D/max-2500 diffractometer, Rigaku Inc.), a diffuse reflectance ultraviolet-visible-near infrared (UV-VIS-NIR) spectrometer (Model CARY 5G, Varian Inc.), a scanning electron microscope (SEM) (S-4300&EDX-350 FE-SEM, Hitachi Co.), and a Fourier transform infrared (FTIR) spectrometer (Spectrum GX, PerkinElmer Inc.).

The N-TiO_2 powder was coated on the inner wall of Pyrex tubes by following the procedure used by a previous study [22]. Ground N-TiO_2 powder (0.5 g) was added to 2 ml of 0.1 mol/L ethylenediaminotetraacetic acid solution. This mixture was diluted slowly by adding deionized water (1 ml) and Triton X-100 (0.1 ml). The resulting paste was smeared onto the Pyrex reactor. The reactor was placed in a dry oven at 100 °C for 0.5 h. Subsequently, the reactor was calcined in a furnace at 350 °C for 0.5 h.

1.2 Activity measurement

The photocatalytic reactor consisted of two Pyrex tubes with different diameters but the same length (26.5 cm, Fig. 1). A conventional lamp or three chips of LED bars arranged in a triangular prism shape was inserted inside the smaller Pyrex tube. The reactor was constructed to increase air turbulence inside the reactor by directing the flow of incoming air towards the light. A standard gas (0.001%) was prepared

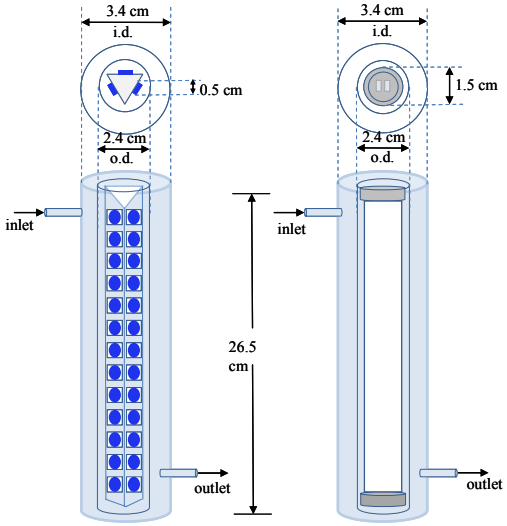

Fig. 1. Schematic of photocatalytic reactor. (a) LED reactor; (b) Conventional lamp reactor.

by injecting standard benzene, toluene, ethyl benzene, or xylene into a mixing system by a programmed syringe pump (model 210, KdScientific Inc.). The reactant gas was directed into the annular region between two Pyrex tubes. The humidity level was controlled using zero grade air and a humidifying device in a water bath (HAAKE W26, Cole-Parmer Inc.). Flow rates were controlled by rotameters.

Photocatalytic activities were evaluated under various operational conditions. The calcination temperatures tested were 350, 450, 550, and 650 °C. One conventional lamp (8 W fluorescent daylight lamp) or five visible 2.16 W LEDs (blue, white, green, yellow, and red LEDs from ItsWell Co., Korea) with a size of 0.5 cm × 0.5 cm and an irradiation angle of 120° were tested. Electric power was supplied to provide three different light intensities (0.26, 1.05, 1.28, and 2.25 mW/cm^2) from the LEDs. The input concentrations used were 0.000005%, 0.00001%, 0.00003%, 0.00005%, 0.00007%, and 0.0001%. The other parameters had values as follows: 50%−55% RH, flow rate 0.5 L/min, calcination temperature 350 °C, violet LEDs, light intensity 2.25 mW/cm^2, and initial concentration 0.00001%.

A series of gas composition measurements were performed at both the inlet and outlet of the photocatalytic system before and after turning on the lamp. Gas sampling was carried out using a 5 L Tedlar bag. Subsequently, gas from this Tedlar bag was drawn through a Tenax TA (0.3 g) stainless steel trap using an air sampler (Aircheck Sampler Model 224-PCXR8, SKC). This sampling was done at room temperature (19−24 °C). The gas phase species collected on the Tenax trap were analyzed by a gas chromatograph (4890, Agilent) with a flame ionization detector coupled to a

thermal desorption system (ATD 400, Perkin Elmer).

1.3 Quality control

For quality control, laboratory blank traps and spiked samples were analyzed. Each day, trap contamination was examined by analyzing a laboratory blank trap. In addition, the quantitative response of the analytical instrument was verified by analyzing a spiked external standard. If the response differed by more than ± 10% from that calculated by the calibration, another calibration process was performed. The detection limits of the gasses were between 1.3 and 5.1 μg/m^3.

2 Results and discussion

2.1 Characteristics of N-TiO_2

The characteristics of the N-TiO_2 photocatalysts were examined using various analytical instruments. Figure 2 presents the XRD results of the photocatalysts calcined at four different temperatures. The proportion of the anatase phase decreased as the calcination temperature increased. This result was consistent with previous studies [23,24]. The XRD pattern of N-TiO_2 calcined at 350 °C showed an anatase phase with a distinct peak at 25.4° and a rutile phase with a less distinct peak at 27.4°. However, the nature of the peaks was reversed for N-TiO_2 calcined at 650 °C. The peak positions were nearly same as the values of Degussa P25 TiO_2 powder reported Xiong et al. [25], which was likely due to the low amounts of nitrogen in the N-TiO_2. This pattern was consistent with those of previous studies [23,24].

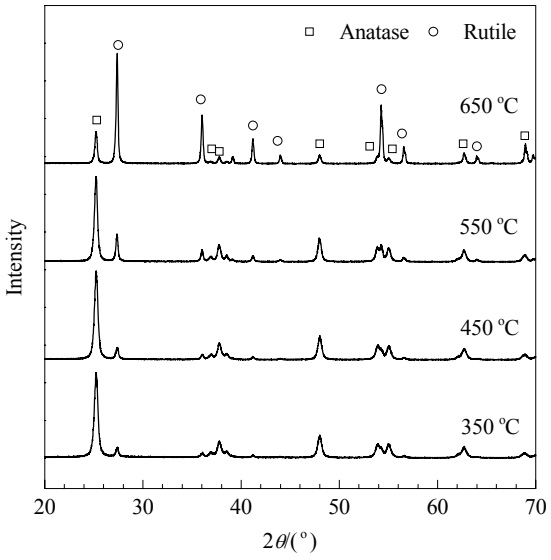

Fig. 2. XRD patterns of N-doped TiO_2 after calcination at different temperatures.

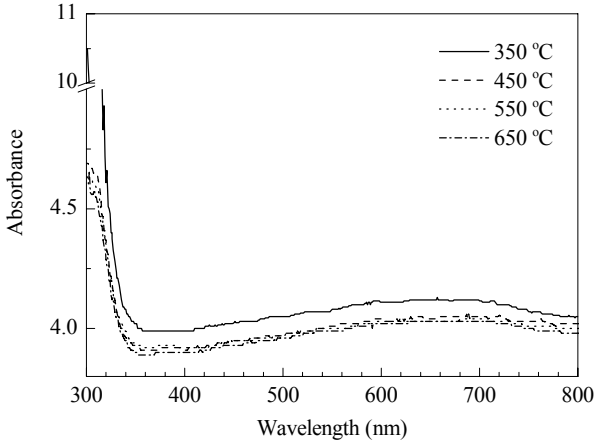

Fig. 3. UV-visible spectra of N-doped TiO_2 after calcination at different temperatures.

Xiang et al [26] have identified the presence of N atoms in the X-ray photoelectron spectrum of a N–S–TiO_2 sample.

Figure 3 shows the UV-visible absorption spectra of N-TiO_2 powder calcined at different temperatures. For the as-prepared powder, the absorbance spectrum was shifted to the visible light region, which agreed with previous studies [23,24]. The absorption edge for this photocatalyst was shifted to $\lambda > 800$ nm, which was ascribed to the N doping. This suggested that the performance of the N-TiO_2 powders can be enhanced under visible light irradiation. The absorption intensities decreased in the descending order of calcination temperatures of 350, 450, 550, and 650 °C, suggesting that the calcination temperature influenced the optical absorption.

The SEM images of N-TiO_2 powders calcined at the four different temperatures are presented in Fig. 4. The sizes of the N-TiO_2 powder were 20, 30, 35, and 40 nm for powders calcined at 350, 450, 550, and 650 °C, respectively. Wang et al. [23] have reported a larger size for N-TiO_2 powder calcined at 600 °C (30 nm) as compared with that at 400 °C (14 nm).

The N-TiO_2 powders calcined at different temperatures gave similar FTIR spectra (Fig. 5). The main absorption peaks were at 3400−3420, 1617−1651, 1060−1064, and < 1000 cm^{-1}. The absorption peaks at 3400 and 1618 cm^{-1} were assigned to the stretching vibration of hydroxyl groups and the bending of adsorbed water molecules, respectively [27,28]. The peak at 1064 cm^{-1} could be due to an interaction between impregnated nitrogen and hydrogen atom, suggesting the successful doping of nitrogen atoms into the TiO_2 [5,24]. Low frequency bands < 1000 cm^{-1} were attributed to the Ti–O–Ti vibration of the network [29,30]. The FTIR results did not show any urea peaks, which are at 3210 cm^{-1} [24]. This suggested that urea species were removed during the washing of the photocatalysts.

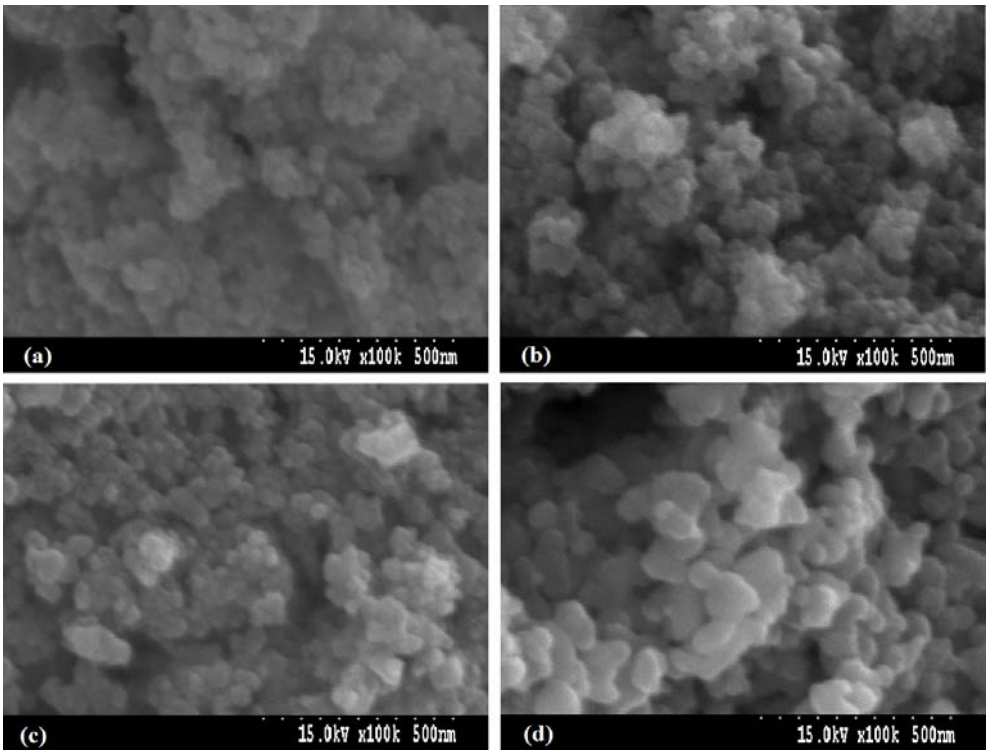

Fig. 4. SEM images of N-doped TiO_2 after calcination at 350 (a), 450 (b), 550 (c), and 650 (d) °C.

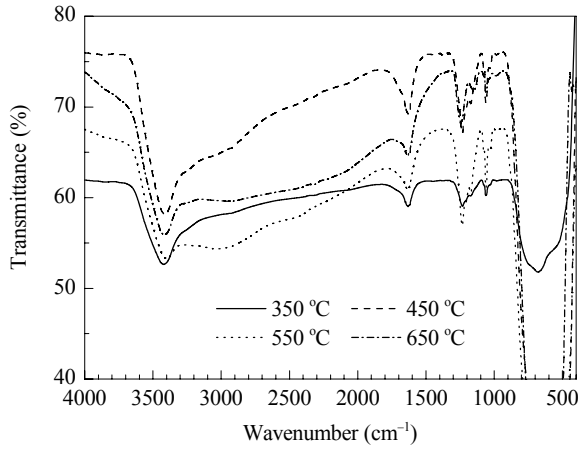

Fig. 5. FT-IR spectra of N-doped TiO_2 after calcination at different temperatures.

2.2 Photocatalytic activity as a function of calcination temperature

The activities of blue-LED irradiated N-TiO_2 photocatalysts as a function of calcination temperature are presented in Fig. 6. Because the degradation efficiency of benzene was close to zero for all calcination temperatures, benzene data were not included in Fig. 6. For the remaining compounds, the degradation efficiency exhibited a decreasing trend with increasing calcination temperature. The highest degradation efficiency was observed at a calcination temperature of 350 °C. The average degradation efficiencies over a 3 h photocatalytic process for toluene, ethyl benzene, *m*-xylene and *p*-xylene, and *o*-xylene were 35%, 68%, 94%, and 93%, respectively. Nosaka et al. [21] have evaluated the photocatalytic activity of a N-TiO_2 photocatalyst for acetone formation and reported that activity decreased with higher calcination temperature. Zhou et al. [31] also reported that the photocatalytic degradation efficiency for toluene was lower for mesoporous TiO_2 nanospheres calcined at a higher temperature (600 °C) than for those calcined at a lower temperature (400 °C), and proposed that this was due to the destruction of the bimodal mesoporous structure of the TiO_2 and decrease of surface area. Matsumoto et al. [5] have evaluated the visible light activity of N-TiO_2 prepared from a layered titania/isostearate nanocomposite by the conversion of aqueous methylene blue and found that above 400 °C within a range of 300−500 °C, visible light activity of N-TiO_2 decreased with increasing calcination temperature.

The photocatalytic activity dependence on calcination temperature of the N-TiO_2 powders was explained by correlating the morphological and optical properties of the photocatalysts. The XRD analysis showed that an increased calcination temperature resulted in a lower anatase content. It has been reported that anatase is superior to rutile as a photocatalyst [32] because the mobility of electrons in anatase is higher than that in rutile due to the lower effective

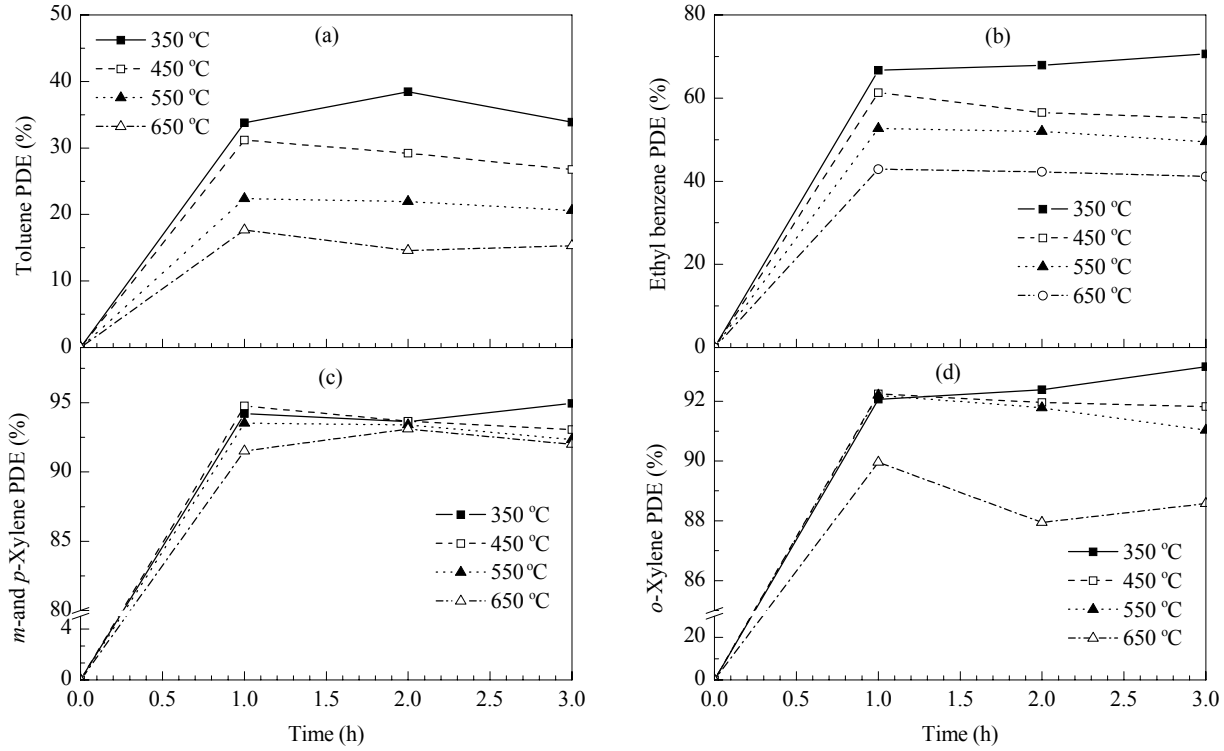

Fig. 6. Photocatalytic decomposition efficiency (PDF) in a photocatalytic system with N-TiO_2 versus calcination temperature.

mass of the electrons, and there is a higher production rate of electron-hole pairs and lower recombination rate in anatase. The SEM images showed that N-TiO_2 powders calcined at a low temperature had a smaller particle size. This is consistent with the finding that the particle size of anatase is smaller than that of rutile, providing it with more photocatalytic surface area [21]. Moreover, N-TiO_2 powder calcined at a low temperature exhibited a higher light absorption intensity. Accordingly, the high photocatalytic activity for low temperature calcined N-TiO_2 powders was ascribable to the higher anatase content, smaller particle size, and higher light absorption intensity. However, the lowering of the calcination temperature of N-TiO_2 powders to too low values would cause poor crystallization [5].

Xylene showed the highest photocatalytic degradation efficiency for all calcination temperatures, and was followed by ethyl benzene, toluene, and benzene in descending order (Fig. 6). The photocatalytic degradation efficiency for benzene was almost zero. This order of degradation efficiency was consistent with that of the photocatalytic reaction rates reported by Strini et al. [33], which suggested that photocatalytic reaction rates are the probable cause for the difference in degradation efficiencies.

2.3 Photocatalytic activity versus light source type

Figure 7 shows the degradation efficiencies in the N-TiO_2 system over three hours according to light source type. The degradation efficiency for benzene was close to zero for all lamps and is not shown. The conventional 8 W fluorescent daylight lamp exhibited a higher photocatalytic decomposition efficiency as compared with that of the LED lamps. The average degradation efficiencies obtained over the 3 h period with the 8 W lamp/N-TiO_2 system were 89% and 95% for toluene and ethyl benzene, respectively, and close to 100% for *m*-xylene, *p*-xylene, and *o*-xylene. Among the LEDs, the white LED gave the highest degradation efficiencies for most of the compounds, followed by the blue, yellow, and red LEDs in descending order. The average degradation efficiencies for the white LED/N-TiO_2 system over 3 h were 36% and 66% for toluene and ethyl benzene, respectively, and close to 100% for both *m*- and *p*-xylene and *o*-xylene. The red LEDs did not show any degradation efficiency for the compounds. Photocatalytic degradation efficiency is proportional to light intensity [34,35]. However, the fluorescent lamp, which exhibited the highest degradation efficiency, had the lowest light intensity when compared to those of the LEDs, except for the red LED (Table 1). This suggested that under the experimental conditions used, light intensity was not an influential parameter in the difference in degradation efficiency between the fluorescent lamp and LEDs. Rather, the wavelength of the fluorescent lamp was distributed in a wide range of 400–720 nm, and had more low wavelengths as compared to those of the

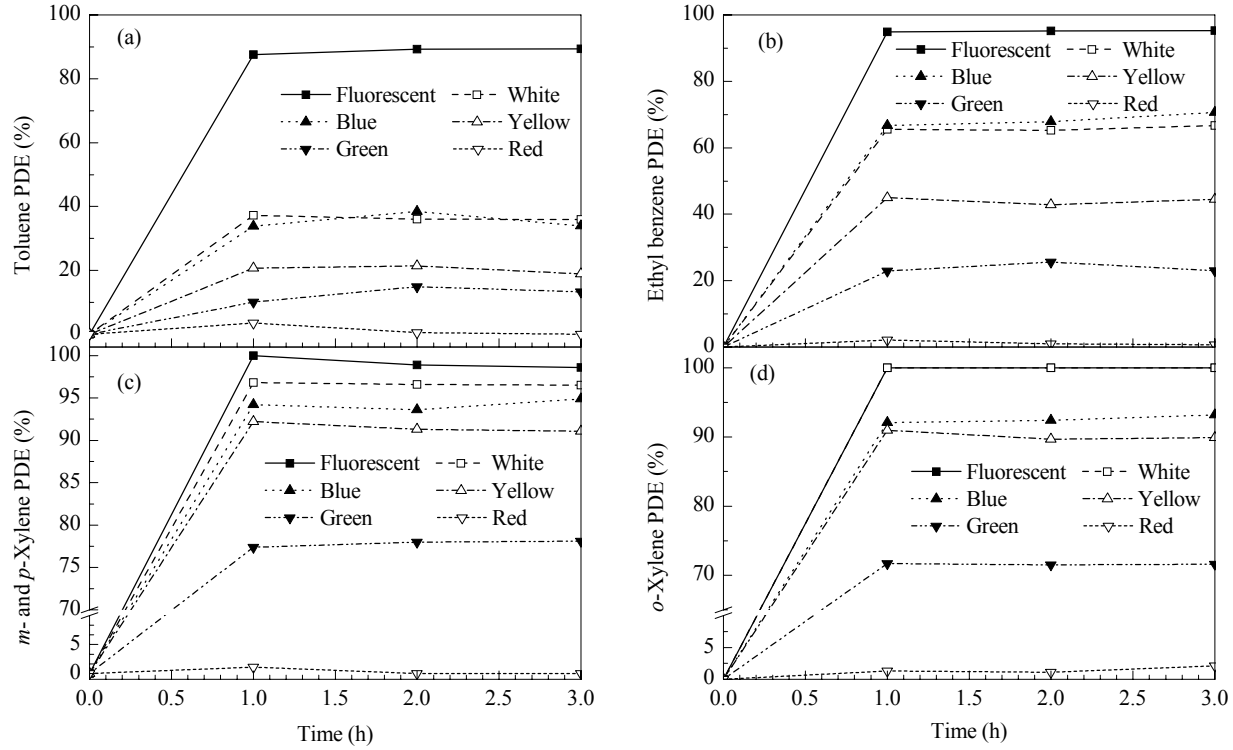

Fig. 7. Photocatalytic decomposition efficiency in a photocatalytic system with N-TiO_2 according to light source type.

Table 1 Peak or range of wavelength, average lamp light intensity, and ratio of photocatalytic degradation efficiency of toluene to power consumption

Lamp	Wavelength (nm)	Light intensity (mW/cm^2)	Ratio (mg/kW)
Fluorescent daylight lamp	400–720	1.2	0.005
White-LED	450	2.3	0.007
Blue-LED	470	2.4	0.007
Green-LED	525	1.5	0.003
Yellow-LED	600–615	1.9	0.004
Red-LED	645–700	0.8	NA*

*Not available.

LEDs. Thus, the higher degradation efficiency for the fluorescent lamp/N-TiO_2 system was most likely due to higher light absorbance by N-TiO_2 powder at low wavelengths (Fig. 3). Similarly, LEDs with a lower peak or range of wavelengths gave higher degradation efficiencies, except for the yellow LEDs, although the white LEDs which have a lower wavelength than that of the blue LEDS had a lower light intensity. In this case, the wavelength effect was likely outweighed by the light intensity effect of the light source. Yellow LEDs with a higher wavelength and light intensity gave a higher degradation efficiency compared with that of green LEDs. The higher degradation efficiency for yellow LEDs suggested that the light intensity effect was likely to outweigh the wavelength effect for photocatalytic degradation. Thus, the degradation efficiency differences between the light sources were attributed to the combined effects of wavelength and light intensity. The light intensities of the LEDs used in this study were different from those used in the Chen et al. study [36]. This difference was attributed to the different LEDs from different companies.

The energy effectiveness of the light source was evaluated by the ratio (R_{EP}, mg/kW) of photocatalytic degradation efficiency to electric power consumption. Toluene was selected for the comparison as this compound is one of the most investigated model pollutants in photocatalytic oxidation studies [37]. These ratios were calculated by the equation used by Shie et al. [19]:

$$R_{EP} = [(c_i - c_0) \times 10^{-3} \times M \times PV/RT]/w \quad (1)$$

where c_i is the DMS input concentration (%), c_0 is the DMS output concentration, M is the DMS molecular mass (g/mol), P is the atmospheric pressure (Pa), V is the reactor volume (L), R is the universal gas constant (0.0083 Pa·L/(mol·K)), T is the absolute temperature in the reactor (K), and w is the power of consumption (kW). In contrast to the photocatalytic degradation efficiencies, the ratios of degradation efficiency to electric power consumption were higher for the photocatalytic systems that used white and blue LEDs than that of the photocatalytic systems that used the conventional fluorescent lamp (Table 1). However, the photocatalytic systems that used blue and yellow LEDs had

lower ratios. This finding confirmed that white and blue LEDs are energy efficient when utilized as light source for photocatalytic conversion of volatile organic compounds (VOCs). However, it is noteworthy that conventional lamps are to be preferred when a higher photocatalytic removal efficiency is needed since the conventional lamp/photocatalytic systems exhibited higher photocatalytic degradation efficiencies compared to those of the LED/photocatalytic systems.

2.4 Photocatalytic activities according to light intensity

The photocatalytic degradation efficiency of TEX increased as the light intensity increased (Fig. 8). This result was consistent with that of Yu et al. [38], who reported an increase in the photocatalytic degradation efficiency of formaldehyde with an increase in light intensity from 0.05 to 2.5 mW/cm^2. A power law is frequently used to describe the light intensity dependency of the photocatalytic degradation rate [39,40]. Light intensity influences photocatalytic activity because the number of photons increases as the light intensity is increased. The photocatalytic reaction rate becomes higher with increasing light intensity according to a first order or half order depending on the light intensity [41]. The light intensity dependence in the range in the present study also followed the power law.

2.5 Photocatalytic activity versus input concentration

The effect of input concentration on degradation efficiency of toluene, ethyl benzene, and xylene is shown in Fig. 9. Similar to the calcination temperature effect, the degradation efficiency of benzene was close to zero for all initial condition. The decomposition efficiency exhibited a decreasing trend with the increase of input concentration. At the lowest input concentration (0.000005%), the average decomposition efficiency over a 3 h period was 40%−97%, while at the highest input concentration (0.0001%) it was 0%−68% depending upon the compounds. Several studies have reported similar trends for other compounds, such as NO_x and VOCs [42−44]. The input concentration dependence was attributed to adsorption competition among the gas molecules for the adsorption sites on the N-TiO_2 surface. At higher input concentrations, the adsorption sites on the photocatalyst surface were not enough for the adsorption of gas molecules. This can be explained with the Langmuir-Hinshelwood adsorption isotherm, which is widely utilized to describe the change in the photocatalytic reaction rate of VOCs with input concentration [34]. According to the Langmuir-Hinshelwood model, the decreasing trend in degradation efficiency with the increase of input concentration suggested that the concentration range tested in the present study was in the intermediate regime or the high

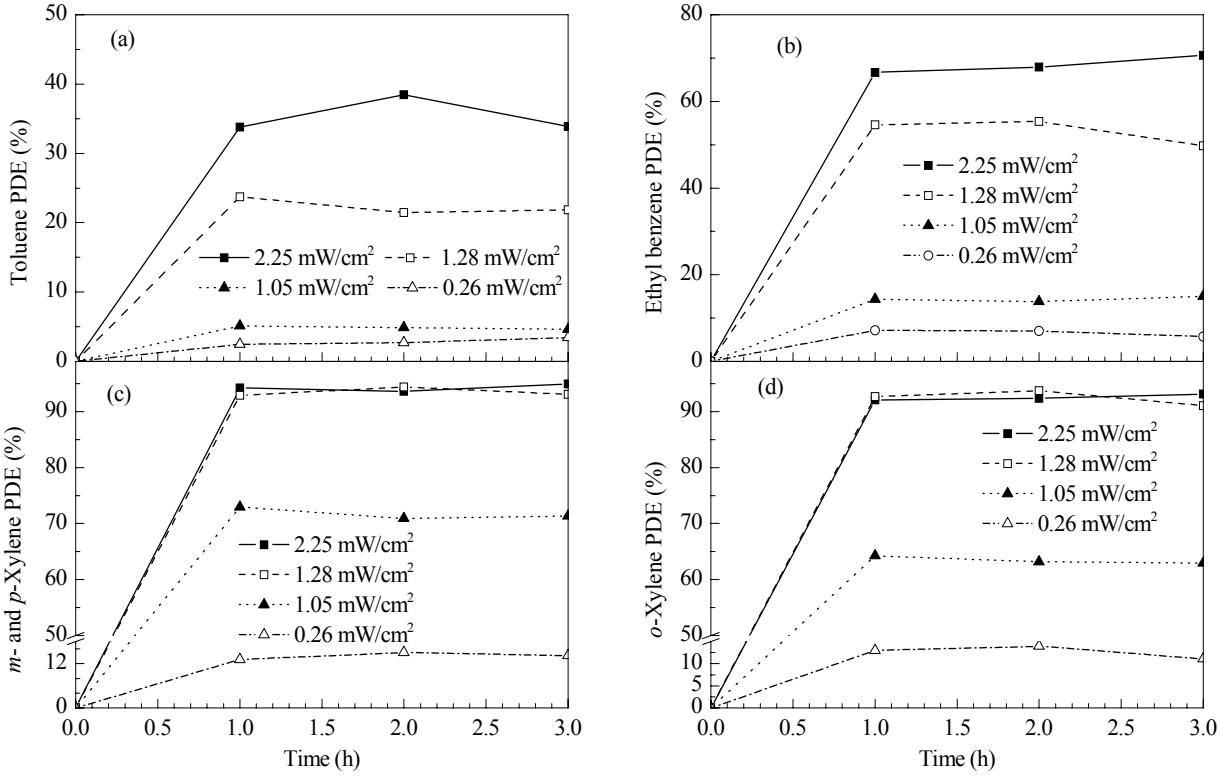

Fig. 8. Photocatalytic decomposition efficiency in a photocatalytic system with N-TiO_2 versus light intensity.

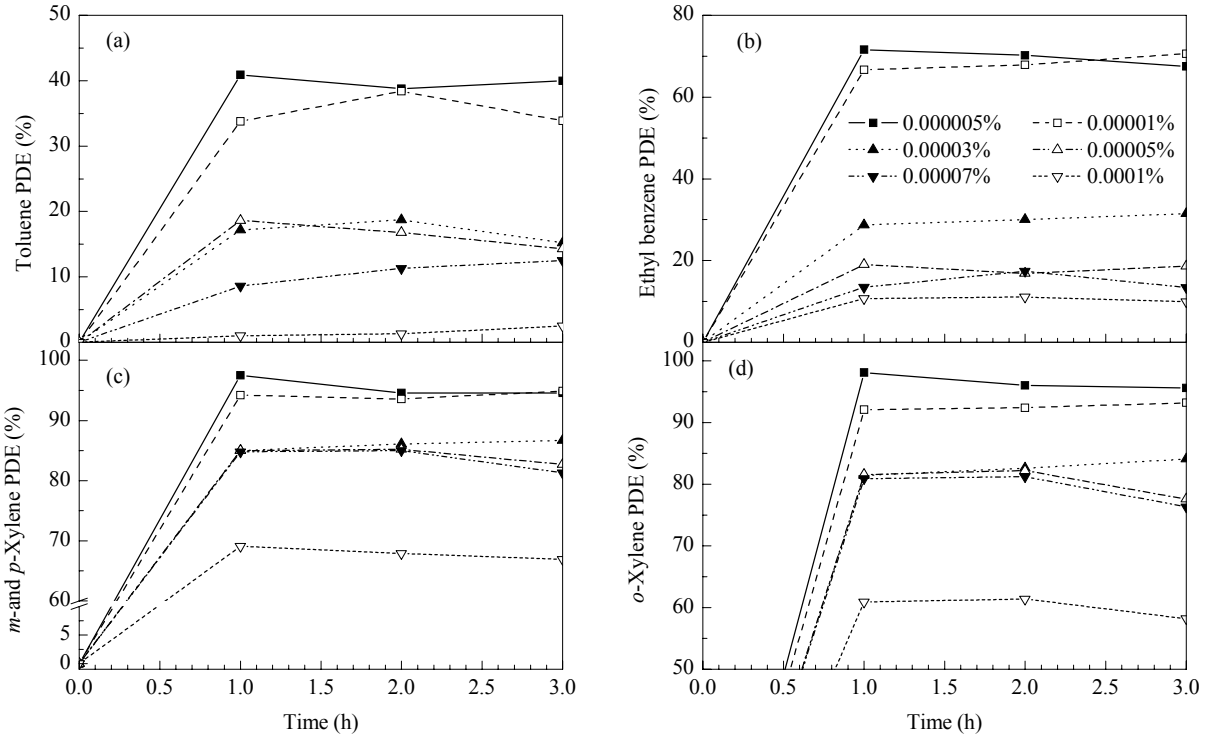

Fig. 9. Photocatalytic decomposition efficiency in a photocatalytic system with N-TiO_2 versus input concentration.

regime, respectively, in which photocatalytic oxidation rate increased slowly but degradation efficiency decreased, or photocatalytic oxidation was independent of input concentrations (zero order reaction kinetics) but degradation efficiency decreased.

3 Conclusions

Chips of visible-LEDs are energy efficient when applied to irradiate N-TiO_2 photocatalyst prepared by the hydrolysis method for the decomposition of gas phase monocyclic aromatics. Although the photocatalytic degradation efficiency was higher with a conventional 8 W daylight lamp irradiated photocatalytic unit as compared to the visible-LED irradiated photocatalytic units, the ratio of degradation efficiency to electric power consumption was higher for some LED-irradiated photocatalytic units (blue- and white-LED irradiated photocatalytic units). Four parameters (calcination temperature, light source type, light intensity, and initial concentration) should be considered when applying LED lamps to the photocatalytic technology for better photocatalytic activity. The morphological and optical properties of the photocatalysts explained the dependence of photocatalytic activity on calcination temperature.

References

1 Herrmann J-M, Duchamp C, Karkmaz M, Hoai B T, Lachheb H, Puzenat E, Guillard C. *J Hazard Mater*, 2007, **146**: 624
2 Xu J, Wang W, Shang M, Gao E, Zhang Z, Ren J. *J Hazard Mater*, 2011, **196**: 426
3 Gaya U I, Abdullah A H. *J Photochem Photobiol C*, 2008, **9**: 1
4 Paz Y. *Appl Catal B*, 2010, **99**: 448
5 Matsumoto T, Iyi N, Kaneko Y, Kitamura K, Ishihara S, Takasu Y, Murakami Y. *Catal Today*, 2007, **120**: 226
6 Peng Y-P, Lo S-L, Ou H-H, Lai S-W. *J Hazard Mater*, 2010, **183**: 754
7 Seabra M P, Miranda Salvado I M, Labrincha J A. *Ceram Int*, 2011, **37**: 3317
8 Chatterjee D, Dasgupta S. *J Photochem Photobiol C*, 2005, **6**: 186
9 Asahi R, Morikawa T, Ohwaki T, Aoki K, Taga Y. *Science*, 2001, **293**: 269
10 Di Valentin C, Finazzi E, Pacchioni G, Selloni A, Livraghi S, Paganini M C, Giamello E. *Chem Phys*, 2007, **339**: 44
11 Peng F, Cai L, Yu H, Wang H, Yang J. *J Solid State Chem*, 2008, **181**: 130
12 Janus M, Choina J, Morawski A W. *J Hazard Mater*, 2009, **166**: 1
13 Jo W K, Kim J T. *J Hazard Mater*, 2009, **164**: 360
14 Wikipedia, Light-emitting diode, 2011. Accessed at http://en.wikipedia.org/wiki/Light-emitting_diode (accessed 07.02.11)
15 Ran J, Yu J, Jaroniec M. *Green Chem*, 2011, **13**: 2708
16 Yu J, Ran J. *Energy Environ Sci*, 2011, **4**: 1364
17 Chen H-W, Ku Y, Irawan A. *Chemosphere*, 2007, **69**: 184
18 Ghosh J P, Sui R, Langford C H, Achari G, Berlinguette C P. *Water Res*, 2009, **43**: 4499

19 Shie J-L, Lee C-H, Chiou C-S, Chang C-T, Chang C-C, Chang C-Y. *J Hazard Mater*, 2008, **155**: 164
20 Liu Y, Liu J, Lin Y, Zhang Y, Wei Y. *Ceramics Int*, 2009, **35**: 3061
21 Nosaka Y, Matsushita M, Nishino J, Nosaka A Y. *Sci Technol Adv Mater*, 2005, **6**: 143
22 Xagas A P, Androulaki E, Hiskia A, Falaras P. *Thin Solid Films*, 1999, **357**: 173
23 Wang Z, Cai W, Hong X, Zhao X, Xu F, Cai C. *Appl Catal B*, 2005, **57**: 223
24 Liu S, Chen X, Chen X. *Chin J Catal*, 2006, **27**: 697
25 Xiong L, Sun W, Yang Y, Chen C, Ni J. *J Colloid Interf Sci*, 2011, **356**: 211
26 Xiang Q, Yu J, Jaroniec M. *Phys Chem Chem Phys*, 2011, **13**: 4853.
27 Geng J, Yang D, Zhu J, Chen D, Jiang Z. *Mater Res Bull*, 2009, **44**: 146
28 Araña J, Doña-Rodríguez J M, Portillo-Carrizo D, Fernández-Rodríguez C, Pérez-Peña J, González Diaz O, Navío J A, Macias M. *Appl Catal B*, 2010, **100**: 346
29 Peng T, Zhao D, Dai K, Shi W, Hirao K. *J Phys Chem B*, 2005, **109**: 4947
30 Wei F, Ni L, Cui P. *J Hazard Mater*, 2008, **156**: 135
31 Zhou M, Yu J, Liu S, Zhai P, Huang B. *Appl Catal B*, 2009, **89**: 160
32 Zhao J, Yang X D. *Build Environ*, 2003, **38**: 645
33 Strini A, Cassese S, Schiavi L. *Appl Catal B*, 2005, **61**: 90
34 Demeestere K, Dewulf J, Van Langenhove H. *Crit Rev Environ Sci Technol*, 2007, **37**: 489
35 Liu B, Zhao X. *Electrochim Acta*, 2010, **55**: 4062
36 Chen Y, Lu A, Li Y, Yip H Y, An T, Li G, Jin P, Wong P K. *Chemosphere*, 2011, **84**: 1276
37 AFNOR, XP-B44-013 Standard, in Photocatalysis: Test & Analysis Method for Determining the Efficiency of Photocatalytic Systems for Eliminating VOC/Odours in Recirculating Indoor Air-Confined Chamber Test, 2009.
38 Yu H, Zhang K, Rossi C. *Indoor Built Environ*, 2007, **16**: 529
39 Wang W, Ku Y. *J Photochem Photobiol A*, 2003, **159**: 47
40 Lim T H, Kim S D. *Chemosphere*, 2004, **54**: 305
41 Kim S B, Hong S C. *Appl Catal B*, 2002, **35**: 305
42 Zhang P Y, Liang F Y, Yu G, Chen Q, Zhu W P. *J Photochem Photobiol A*, 2003, **156**: 189
43 Hegedüs M, Dombi A. *Appl Catal B*, 2004, **53**: 141
44 Yu Q L, Brouwers H J H. *Appl Catal B*, 2009, **92**: 454